

## EVALUATION OF GEOMETRIC PARAMETERS OF THE STOMATOGNATHIC SYSTEM USING RADIOLOGICAL IMAGING

Wojciech Ryniewicz<sup>1</sup>), Łukasz Bojko<sup>2</sup>), Anna M. Ryniewicz<sup>2</sup>)

1) Jagiellonian University Medical College, Faculty of Medicine, Dental Institute, Department of Dental Prosthodontics and Orthodontics, 4 Montelupich Street, 31-155 Krakow, Poland ([wojciechj@ryniewicz.pl](mailto:wojciechj@ryniewicz.pl))

2) AGH University of Science and Technology, Faculty of Mechanical Engineering and Robotics, 30 Mickiewicza Ave., 30-059 Krakow (✉ [lbojko@agh.edu.pl](mailto:lbojko@agh.edu.pl), +48 12 6173 521, [anna@ryniewicz.pl](mailto:anna@ryniewicz.pl))

### Abstract

In modern clinical practice in various areas of dentistry, there is a need to virtualize and determine the diagnostic parameters of the stomatognathic system (SS). The aim of this article is to provide an evaluation of correct SS structures based on a comparison of mappings in pantomography, lateral cephalometry, and volumetric tomography using bone and tooth anthropometric points. The digital measurements performed determine the applicability of the analyzed imaging techniques for clinical diagnostics by indicating discrepancies and errors in the evaluation of geometric parameters. They should verify the location of characteristic points, lines, angles, and planes in relation to spatial objects mapped on the 1:1 scale. The analyses performed confirm the appearance of bone and dental structure asymmetry in healthy patients.

Keywords: pantomography, cephalometry, CBCT, craniofacial, biometrology.

© 2022 Polish Academy of Sciences. All rights reserved

## 1. Introduction

To identify the structures of the *stomatognathic system* (SS) and to indicate the diagnostic possibilities, the following extraoral radiological examinations are performed: pantomography, lateral cephalometry, and *cone beam computed tomography* (CBCT) [1–7]. The literature compares most often two selected imaging techniques: cephalometry and CBCT [3,4] or cephalometry and MRI [6] and CBCT and MRI [1] used to indicate the characteristic points or diagnostics focused on a specific pathology of SS. An interesting study is the identification of the menton (Me) on posteroanterior cephalograms and in 3D CBCT, because the midpoint of the symphyseal area is not identifiable after the mandibular symphysis fuses at an early age. The aim of this study was to evaluate the reliability of the identification of the *genial tubercle* (GT) in patients with mandibular asymmetry and to compare it with that of the traditional landmark (Me). The results suggest that both Me and GT are clinically reliable and equally useful landmarks for the evaluation of mandibular asymmetry in CBCT images [4]. Of note is the prospective study to evaluate whether magnetic resonance imaging is equivalent to lateral cephalometric radiographs. The applied MRI technique

has been optimized for short scanning time, high resolution, high contrast, and geometric accuracy. The data sets have been transformed into lateral cephalograms, allowing reliable measurements as applied in orthodontic routine of high concordance with the corresponding measurements in cephalometry. This study shows the feasibility of planning orthodontic treatment based on MRI, without exposure to radiation [6]. Another interesting item is the evaluation of combined cone beam tomography and magnetic resonance images used to evaluate the position of the articular discs. The fusion of these images significantly improved the reliability of evaluation due to high resonance resolution for soft tissue examination. The temporomandibular joint has a layered structure. In this study, it was particularly important to map and location of the articular disc and the articular surfaces made of fibrous cartilage [1]. Patients often require combined treatment involving different areas of dentistry. In dental prosthetics, orthodontics, endodontics, implanto-prosthetics, and surgery, it is necessary to determine the correlated diagnostic parameters of the stomatognathic system because they can optimize the treatment process [2–4,8,9]. The holistic approach to treatment allows for correct occlusion and full face aesthetics, and complications in the form of periodontal disorders, temporomandibular joints, and recurrences often result from insufficient diagnosis. The SS geometric parameters are used to determine mathematical correlations between the measurement values, allowing the standardization of the results and the elimination of subjective error of the assessor. They make it possible to determine deviations from the norm and also to define the direction of treatment and its priorities. The basic principle of all diagnostic analyzes is the possibility of finding points and repeatability of measurements, by one researcher as well as many researchers of them. Established norms may serve the population in which the studies were conducted, but may not be appropriate for other populations. For this reason, many clinicians create their own analyzes, which are a set of selected measurements, used in the diagnostics of their patients. Therefore, studies were carried out that will be compared with the variables expected for the type of face of a given patient treated at the Krakow University Dental Clinic.

At the same time, the ALARA principle, which must be observed, means that the largest possible amount of diagnostic information should be obtained at the maximum reduction in radiation dose [10]. The 3D imaging technique offers new possibilities of diagnosis and treatment. The use of CBCT is an alternative to traditional CT. It has a much lower radiation dose and lower costs of image recording. The doses of ionizing radiation in radiological imaging in dentistry are as follows: analog pantomography – 26  $\mu$ Sv, digital pantomography – 4.7  $\mu$ Sv, spiral CT (classic) – 1700 ÷ 3000  $\mu$ Sv and CBCT – 35 ÷ 90  $\mu$ Sv [9, 11].

The aim is to evaluate the correct SS structures based on the comparison of mappings in pantomography and lateral cephalometry, which give a 2D back projection, and volumetric tomography, which enables a spatial reconstruction of the studied subject. Anthropometric points according to Steiner were used for the imaging analysis. The medical criterion is to indicate the possibility of locating even and odd anthropometric points and to compare the position of the located points and the distances determined on their basis in the craniofacial area tested using the above mentioned methods. The measurements performed indicated discrepancies in the evaluation of the geometric parameters of the stomatognathic system resulting from the applied imaging technique, which must be taken into account in the clinical procedures performed. The imaging techniques with the use of the ball standard were subjected to metrological evaluation.

## 2. Material and methods

The materials used for the study were pantomographic, lateral cephalometric and CBCT imaging results carried out in 20 healthy men (aged  $25 \pm 3$  years) at the University Dental Clinic in Krakow in the Image Diagnostics Laboratory. The research group consisted of men without

disorders and malocclusion, as well as skeletal disproportions. They had the correct parameters of occlusion and good condition of the teeth. The consent of the Bioethics Committee was obtained to carry out such research (decision number KBET/89/B/2009).

The study method involved radiological examination using the three techniques mentioned above in each of the patients and an indication of the diagnostic options representative of such techniques. In all studies, procedures and recommendations related to patient protection, his location, and the introduction of appropriate imaging parameters were followed.

Clinical imaging systems are quality controlled according to international standards or national recommendations. In Poland, these provisions are included in the Regulation of the Minister of Health of December 24, 2002. The regulations apply to health care facilities that use devices which use ionizing radiation. According to the Minister's recommendation, the Clinic conducts periodic internal quality control tests of devices used in radiological diagnostics.

The controls were performed using a phantom, which is a standard containing elements made of materials with values in *Hounsfield units* (HU) corresponding to the gray level of human tissues.

For a selected group of patients, panoramic imaging was performed with the use of a ProMax® radiographic unit (Planmeca, Helsinki, Finland 2005) at 74 kVp and 10 mA. In standard pantomography, many factors affect the quality of the image and its diagnostic value: patient positioning, motionless position during examination, imaging parameters, and the angle at which the beam reaches the sensor. The differences in the grayness of structures are caused by the differences in the absorption of ionizing radiation, while the overlapping of many structures, both bones and soft tissues, in the studied object results in back projection. Depending on the angle of the beam reaching individual stomatognathic system structures, they may introduce a significant distortion of the form. Another diagnostic procedure applied was lateral cephalometric projection. Cephalometric examinations were performed using the Planmeca ProMax Helsinki Finland device with the application of additional equipment – special arms attached to the pantomographic device. The enlargement in the examinations in question was 10%. The Frankfurt plane was parallel to the ground level, while the midsagittal plane of the head was parallel to the cassette in a vertical position. The central beam passed through the external acoustic opening. Cephalometric tests were performed at the following parameters: 90 kV, 12 mA, 16 s and 54 mGy.

Then, a selected group of patients underwent CBCT using RAY Scan Symphony tomography with the following *field of view* (FOV): 10 × 10 cm, 15 × 15 cm and 17 × 23 cm, with an expanded field of the view mode. During the procedure the patient was seated, the head was fixed, and the Frankfurt plane was parallel to the ground level. The short time of the examination, which lasted 26.9 s, minimized motor artifacts. The dose of radiation was similar to the one used for an extraoral point picture and equaled 36–74 μSv. The examination was carried out with parameters of the voxel size of 380 × 380 × 380 μm. On the basis of CBCT imaging, spatial reconstructions of the craniofacial area of the examined patients were performed.

The implementation of the research program was preceded by individual calibration of the devices, which resulted from previous measurement experiences [12]. To ensure the correct metrological evaluation of imaging systems, an uncertainty analysis was carried out in accordance with the guidelines of VDI/VDE 2630 and related standards ASTM E1441-19 and ISO 10360, which characterize parameters in four groups related to: length measurement error, scanning error, dimensional shape dependencies and resolution. The tests were carried out using a standard zirconium ball with a diameter of 1/2" and class 0. The ball was stabilized on a special base in the central area of the patient's head. The precision of the mapping was evaluated by comparing the reconstructed models, based on 20 measurements in each imaging technique: pantomography, lateral cephalometry, and CBCT tomography, with the geometric parameters included in the ball

certificate. The comparison was carried out using the best-fit method using the 3D Reshaper program. The standard uncertainty determined by Method A was 0.40 mm for pantomography, 0.32 mm for lateral cephalometry and 0.10 mm for CBCT.

Geometric comparison of representations in pantomography, lateral cephalometry and CBCT was carried out using classification points according to skeletal classes (Table 1). The points taken

Table 1. Description of points used in measurements of the stomatognathic system, the basis for Steiner classification [9].

Points	Definitions
Sella (S) /odd/	The midpoint of the sella turcica; it is located in the midsagittal plane
Nasion (N) /odd/	The most anterior point on the frontonasal suture
Porion (Po) /even/	The upper- and outer-most point on the external auditory meatus
Orbitale (Or) /even/	The most interior and anterior point on the orbital margin at the intersection of the pupil line (a vertical line crossing the middle of the pupil) when looking straight ahead with the lower edge of the orbit
Articulare (Ar) /even/	The point of the intersection of the posterior margin of the ascending mandibular ramus and the outer margin of the posterior cranial base
Gnathion (Gn) /odd/	The most anterior and interior point on the bony chin
Menton (Me) /odd/	The most inferior point of the mandibular symphysis in the midline
Pogonion (Pog) /odd/	The most anterior point on the bony chin
Gonion (Go) /even/	The point of the intersection of the mandibular line with the line adjacent to the mandible ramus; the mandibular line crosses Gn and the inferior mandibular angle bulge; the line adjacent to the mandibular ramus crosses Ar and the posterior mandibular angle bulge
Point A (Subspinale) /odd/	The deepest point on the curved profile of the maxilla between the anterior nasal spine and the alveolar crest
Point B (Supramentale) /odd/	The deepest point of the curved profile of the mandible between the chin and the alveolar crest
Anterior nasal spine (ANS) /odd/	The tip of the bony anterior nasal spine in the midline
Posterior nasal spine (PNS) /odd/	The point of intersection of the posterior contour of the maxilla body (anterior limitation of the pterygopalatine) with the contour of the hard or soft palate (may be covered by erupting molars)
Incisor superius (Is) /odd/	The tip of the crown of the most anterior maxillary central incisor
Upper incisor apex (UIA) /even/	The root apex of the most anterior maxillary central incisor
Incisor inferius (Ii) /odd/	The tip of the crown of the most anterior mandibular central incisor
Lower incisor apex (LIA) /even/	The root apex of the most anterior mandibular central incisor
Molar superioris (Ms) /even/	The mesial cusp tip of the maxillary first molar
Molar inferioris (Mi) /even/	The mesial cusp tip of the mandibular first molar
Condylion (Cd) /even/	The most lateral point on the surface of the head of the mandible

into account were those determined in the panoramic radiograph and the lateral cephalogram (characteristic of these projections) and the points determined in the spatial reconstruction on the basis of CBCT that were characterized by a geometric representation of anatomical location.

To compare these three imaging techniques, a midsagittal plane was introduced. The characteristic distance of points for pantomography and CBCT was evaluated in relation to this plane. The location of characteristic points and linear dimensions between the points in cephalometry and in CBCT was also controlled in relation to this plane. Additionally, the spatial location of the selected even points in the orthogonal system was analyzed on the basis of CBCT. Cross-sections were also performed in the midsagittal plane and in selected sagittal planes crossing the anthropometric points that were analyzed in pantomographic and cephalometric examinations.

### 3. Test results and their analysis

The edge of the midsagittal plane, together with some odd points belonging to it (Fig. 1), was determined on pantomographic examinations. Not all the characteristic points of this plane could be marked on a panoramic radiograph. On the basis of CBCT, in the midsagittal cross-section it was also possible to indicate the remaining characteristic points that were overshadowed in the panoramic radiograph (Fig. 1 and 4). The way of positioning the patient and the necessity to select automatic projections, image enlargement, and deformation of anatomical structures make it impossible to perform objective measurements on the basis of a panoramic radiograph.

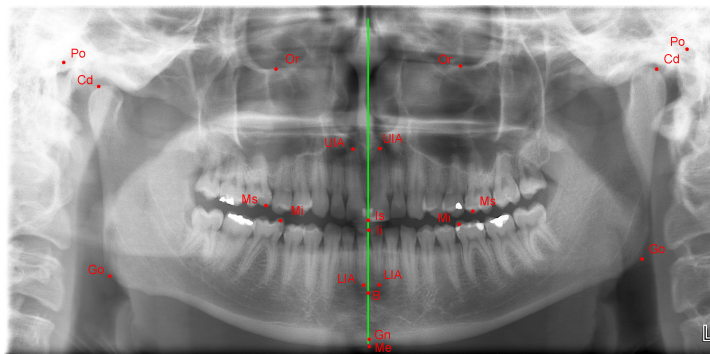


Fig. 1. A panoramic radiograph with the defined edge of the midsagittal plane and characteristic points: Me, Gn, Ia, and Is.

The points identified in the cephalometric analysis were the odd points: Me, Gn, Ia, and Is, which define the midsagittal plane, and the even points: Uia, Uia, Mi, MS, Go, Cd, and Po, which lie outside this plane and could be identified (Fig. 2).

Spatial reconstructions were prepared on the basis of CBCT results using Xelis Dental software. Anthropometric points were determined on 3D reconstructions of craniofacial bone structures. Their location was a consequence of their objective shape and they were defined in Steiner classification as reference points (Table 1, Figs. 3 and 4). Based on these points in the midsagittal plane, 8 measurement sections were identified: *Nasion-Sella* (NS), Distance between points A and Gn (A–Gn), Palatal length (ANS–PMS), Lower face height (ANS–Me), Distance between points N and Me (N–Me), Facial plane (N–Pog), Distance between points A and Pog (A–Pog), Distance between points N and B (N–B) (Fig. 5). Section linear measurements were made using

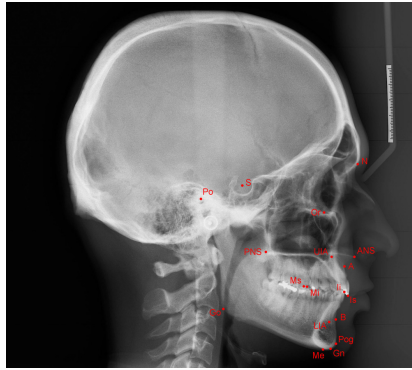


Fig. 2. Cephalogram with location of the reference points in Steiner analysis.

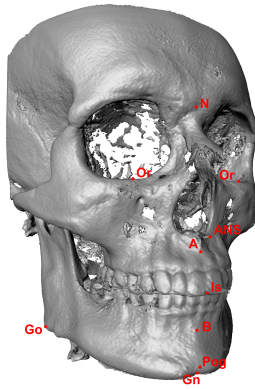


Fig. 3. Craniofacial bones reconstructed on the basis of CBCT with marked reference points.

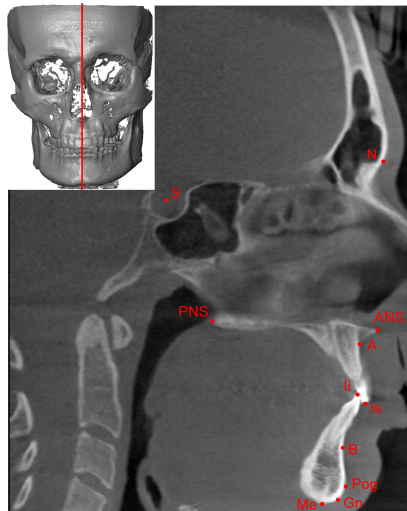


Fig. 4. A cross-section in the midsagittal plane on the basis of CBCT with the following odd points marked: N, S, PNS, ANS, A, Ii, Is, Pog, Gn and Me, B.

digital methods *i.e.*, Photoshop CS2 for lateral cephalometry, Adobe and Xelis Dental for CBCT. The appropriate sections measured in the research group of patients with both imaging techniques applied were characterized by an approx. 20% dispersion of the results. Such dispersion originates from differences in the anatomical structure of patients in the evaluated group.

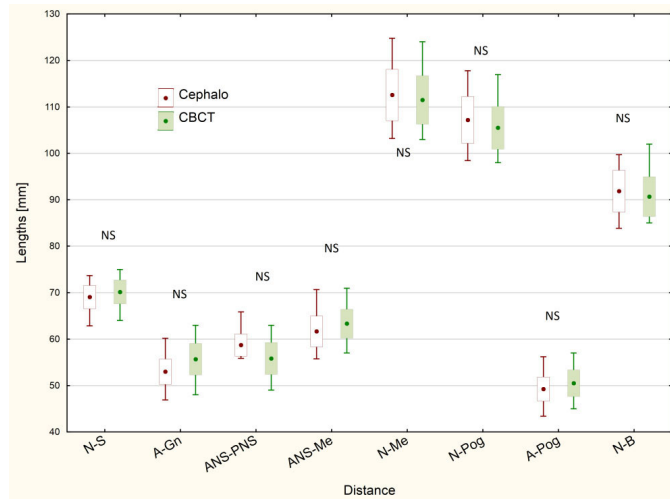


Fig. 5. Distances between selected odd points in cephalometry and CBCT.

Calculations were performed using the Statistica 13.1 package. The distances between the anthropometric odd points lying in the midsagittal plane were characterized by the parameters of descriptive statistics: the mean value, the standard deviation, and the dispersion of the test results (Fig. 5). In the second stage, normality tests were performed for each group of distances with the Shapiro-Wilk test. Not all results groups had a normal distribution (Shapiro-Wilk test  $p > 0.05$ ). In the next stage of statistical analyzes, the U-Man Whitney test was performed which showed no significant statistical differences between the lengths tested in all imaging techniques. Statistical values were tested at the significance level of  $p < 0.05$ .

For comparison, based on imaging and reconstruction with CBCT, the location of even anthropometric points in sagittal planes crossing the following points was presented: the root apex of the most anterior mandibular central incisor LIA (Fig. 6a), the root apex of the most anterior maxillary central incisor UIA (Fig. 6b), the mesial cusp tip of the mandibular first molar – Mi (Fig. 7a) and the point of the intersection of the mandibular line with the line adjacent to the mandible ramus – Go (Fig. 7b).

To further illustrate the method on the basis of the CBCT results obtained, an analysis of the spatial locations of anthropometric even points Mi, MiR on the right, and MiL on the left, was carried out. For a group of 20 patients examined, it was found that in the frontal plane projection, there is an asymmetry in the position of the points in relation to the midsagittal plane (Table 2). This information led the authors to perform a deeper analysis which consisted of identifying the location of the Mi points for a randomly selected patient. For 3D reconstruction with CBCT, an orthogonal coordinate system xyz was introduced (Fig. 8). This system specifies the coordinates of the MiR and MiL points. The repeatability of CBCT diagnostics was evaluated by determining the standard deviation of the measurements determined by the coordinates of the selected even point on the basis of a series of 20 measurements. The analysis of the spatial location of even

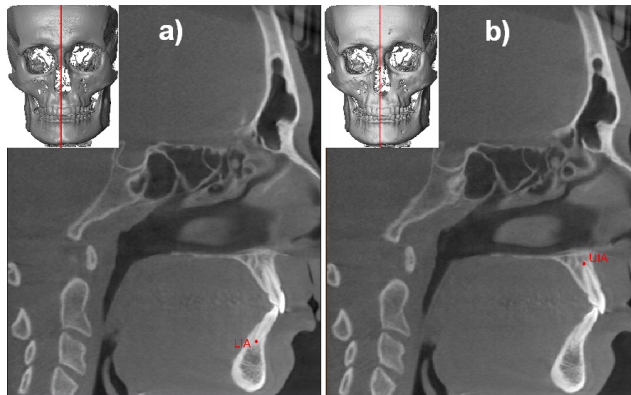


Fig. 6. Sagittal cross-sections based on CBCT crossing the following even points: a) the root apex of the most anterior mandibular central incisor LIA, b) the root apex of the most anterior mandibular central incisor UIA.

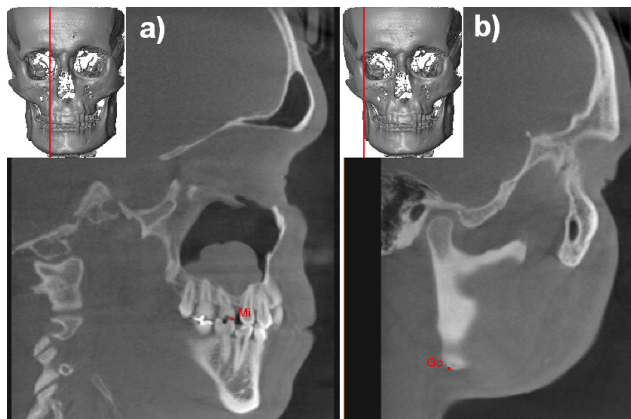


Fig. 7. Sagittal cross-sections on the basis of CBCT on the right crossing the following even points: a) the mesial cusp tip of the mandibular first molar – Mi, b) the point which determines the mandibular angle – Go.

points Mi on the right and left indicates that they have different locations, both in the horizontal and frontal planes. This confirms the asymmetry of the right side in relation to the left side. Due to this asymmetry of the location of MiR and MiL, the distance between them was determined in a three-dimensional space –  $d(\text{MiR}, \text{MiL})$  (1).

$$d(\text{MiR}, \text{MiL}) = \sqrt{(x_{\text{MiR}} - x_{\text{MiL}})^2 + (y_{\text{MiR}} - y_{\text{MiL}})^2 + (z_{\text{MiR}} - z_{\text{MiL}})^2}. \quad (1)$$

The calculated mean distance between the even anthropometric points Mi on the right side MiR and the left side MiL is 54.69 mm, and the measurement uncertainty determined by the A method is 0.11 mm [13]. Statistical analysis revealed the normal distribution of test results.

In order to determine the asymmetry in the craniofacial structures, in the group of 20 patients, the even bone and dental points were located: LIA, UIA, Mi, Ms, Or, Go, Cd. The measurements were performed taking into consideration the position of these points on the right and on the left sides, in relation to the midsagittal plane, in frontal plane projection. The mean values of the

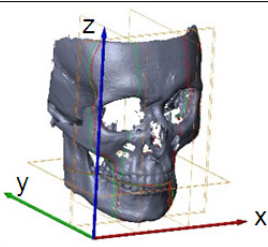
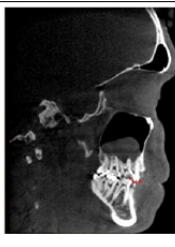
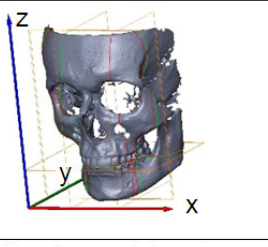
Point	Anatomical area	Sagittal cross-section (yz)	Horizontal cross-section (xy)	Frontal cross-section (xz)
MiR				
	Coordinates of the point, mm	$X_{MiR} - 51,6$	$Z_{MiR} - 44,8$	$Y_{MiR} - 49,6$
	Standard deviation, mm	0,14	0,11	0,16
MiL				
	Coordinates of the point, mm	$X_{MiL} - 106,0$	$Z_{MiL} - 42,6$	$Y_{MiL} - 44,4$
	Standard deviation, mm	0,18	0,20	0,19

Fig. 8. Determination, based on CBCT, of the location of points at the tips of the mesial cusp of the mandibular first molars, MiR on the right and MiL on the left.

Table 2. Distances determined in the group of 20 patients, based on CBCT, between the even points and the midsagittal plane, in the frontal plane projection.

Even anthropometric points		Distance to the midsagittal plane [mm]		Asymmetry in the position of the points, %
		Mean values	Standard deviation	
LIA	R	2.91	1.93	6.99
	L	2.53	1.91	
UIA	R	3.74	1.07	10.63
	L	4.63	0.23	
Mi	R	26.88	4.04	1.63
	L	26.02	4.42	
Ms	R	28.46	3.94	3.05
	L	30.25	4.71	
Or	R	32.60	2.98	3.54
	L	34.99	4.31	
Go	R	50.90	6.26	0.48
	L	51.39	8.08	
Cd	R	63.16	6.87	0.81
	L	64.19	7.43	

distance and standard deviations in the analysed points were determined in relation to the plane (Table 2). The results of the research indicate differences between the positions of the points on the right and left sides in relation to the midsagittal plane, which indicates asymmetry in the anatomical structure of the craniofacial area.

For the group of men studied, there are differences in the mean values of the distances of the points from the plane, ranging from 0.19 mm to 1.79 mm. The percentage asymmetry determined for individual points in the test group was in the range of 0.48% to 10.63%. Note that the greatest asymmetry occurs at the LIA and UIA points. The literature emphasizes that the identification of the position of the upper and lower incisors is particularly problematic. Finding their vertices precisely is often impossible [11].

#### 4. Discussion

In pantomography and lateral cephalometry, the mapping is two-dimensional. This representation is a projection of the evaluated structures upon planes: respectively in the pantomography – on the frontal plane and in the lateral cephalometry – on the sagittal plane. Not all structures are visible because there is back projection and overshadowing caused by the different abilities of the tissues in the image to absorb radiation. To use information from a two-dimensional imaging and make a diagnostic decision, a clinician must have knowledge of the anatomy of the SS and preferably perform CBCT imaging and 3D reconstruction. Pantomography is only a review image, and lack of shape-dimensional mapping and image summation may be misleading in the SS evaluation.

The back projection of anatomical structures and a nonparallel beam in lateral cephalometric make it impossible to determine spatial coordinates of the dental and bone even points and perform a reliable measurement of the distance between them (Fig. 2). In cephalometric diagnostics, the angles defined in orthodontics for the population with normal craniofacial bone development and the population with irregularities are projections in the image plane. A diagnostic inconvenience and perhaps the need for additional imaging is the summation of structures in the midsagittal plane, which causes obscuring and difficulties in locating bone and dental points. Furthermore, in this type of imaging, it is impossible to evaluate craniofacial asymmetry. It would be possible to perform cephalometric imaging from the other direction, but the error in locating anthropometric points would be much greater than in the case of CBCT and its processing would require a specialized program according to the proposed method. Often, also during orthodontic treatment, it is necessary to locate and clinically shift dental structures using biomechanical excitations caused by appropriate appliances. In such situations, it is better to use CBCT diagnostics.

The use of CBCT in the evaluation of diagnostic parameters of the stomatognathic system is a result of the progress and rapid development of digital technologies in radiology. In this examination, multiplane images can be obtained using a cone-shaped beam. It is possible to define any cross-sectional plane and spatial reconstruction while voxels are isotropic [14]. 3D reconstruction can be freely rotated and cut with frontal, horizontal, and sagittal planes as well as any other planes. The vertical position of the head during imaging allows one to scan the natural shape of the soft tissues and eliminates the risk of mandibular retraction.

Efforts are being made to assess whether the cephalogram obtained using the traditional method may be replaced by a cephalogram synthesized from volumetric imaging [15–17]. The latter has many more metrological advantages. Depending on the direction of its preparation compared to the midsagittal plane, the symmetry of the location of characteristic points may be evaluated.

Based on CBCT diagnostics, the determination of the midsagittal platform is reliable due to the ability to identify a number of points (N, S, PNS, ANS, A, Ii, Is, Pog, Gn and Me) that belong to it (Figs. 2 and 4). Moreover, in this plane, it is possible to determine the linear dimensions between odd points. The results of the examinations carried out demonstrated that linear measurements between odd points in the midsagittal plane are not statistically different between the imaging techniques in cephalometry and CBCT (Fig. 5). Similar conclusions have been presented in the reference literature [16, 18–21]. In this case, cephalometric standards can be used to evaluate CBCT in 3D. Until now, the basis for diagnosis and treatment consisted of general orthodontic standards developed by Broadbent in 1931, based on 2D imaging [9].

Various centers have analyzed the determination of the geometric parameters of the stomatognathic system using a variety of imaging techniques [21–25]. CBCT is an especially popular technique as it allows spatial reconstructions and virtual measurements with the smallest margin of error with respect to shape representation [15, 21, 26–28]. The study has shown that in the diagnostic assessment of SS, based on pantomography and cephalometry, there is obscuration of the structure and shape-dimensional deformation.

The presented material uses an original method, based on CBCT imaging, of introducing an orthogonal coordinate system into spatially reconstructed (1:1 scale) research objects and analyzing the location of characteristic points. This method makes it possible to determine their location in the stomatognathic system with an uncertainty of 0.11 mm and perform virtual measurements. The determined values of the distance in the group of 20 examined men allowed to indicate the asymmetry in the location of the even points in relation to the midsagittal plane, in the projection on the frontal plane (Table 2).

Direct measurements on 3D reconstructions on the basis of CBCT give a better differentiation of anatomical structures, and have an advantage over 2D images obtained in traditional cephalometry in which there is summation of the image on the plane and obscuration of structures. A barrier to broad implementation of this diagnostic tool is the fact that the interpretation and geometric criteria, such as angles, lines, and planes defined in cephalometry, have not been defined for spatial structures yet. To be able to compare measurements of three-dimensional objects with those of two-dimensional objects, which are currently applied in clinical practice, it is necessary to create a new set of standards in a 3D system referring to various classes of craniofacial bones in the population. A geometric analysis enables evaluation of the SS at the stage of treatment planning, visualization of treatment results, and their documentation. A digital recording of the reconstruction on the basis of CBCT enables FEM (*finite element method*) strength analysis and the printout of objects before implantoprosthetic and prosthetic surgeries [7]. The significance of spatial mapping of the craniofacial structures and its biometry are evidenced by numerous works and reports related to this problem [1, 15–17, 19, 20, 24, 27].

Objective 3D mapping, which can be obtained based on CBCT, is the basis for preoperative virtual planning of craniofacial reconstructive surgery [29–32]. Assessment of the geometric parameters of the SS is the basis for implantological reconstruction based on a three-dimensional assessment of the shape and quality of the jaw and mandible bones. It allows optimal presurgical positioning of implants in the alveolar bone and the alveolar part of the mandible, as well as correct design of the implantoprosthetic structure [26, 33]. In our research, an analysis of the location of intraosseous implants in the mandible modeled on the basis of CBCT was carried out (Fig. 9). Based on the shades of gray, the density distribution of the mandibular bone was evaluated in the area of implant application, ranging from 2176 HU to –1024 HU (Fig. 9a). The height of the mandible was determined from 26 mm to 31 mm  $\pm$  0.5 mm and the width of the mandible from 8 mm to 14.5 mm  $\pm$  0.5 mm in the area of the planned reconstruction. Three

implants with a diameter of 3.5 mm and a length of 12 mm were selected. The direction of insertion and positioning of the implants were determined.

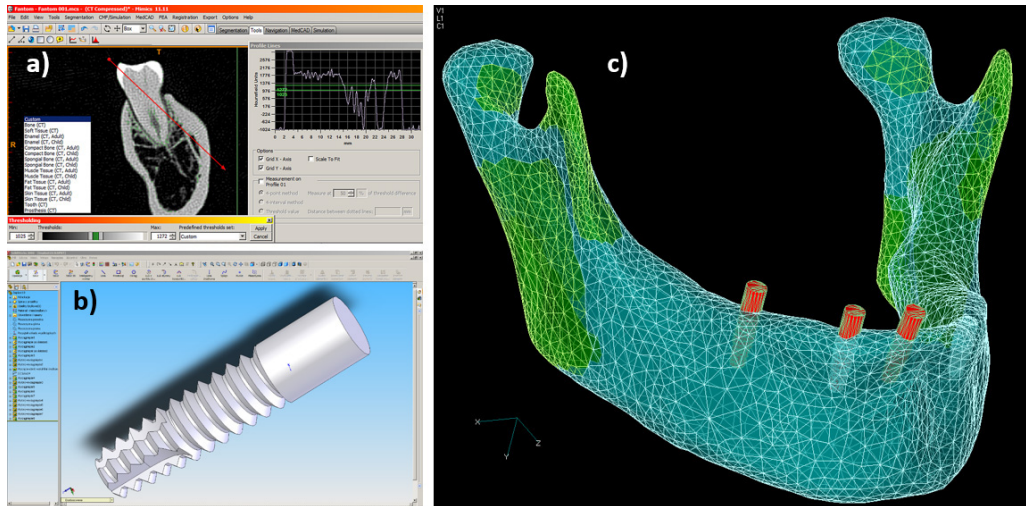


Fig. 9. Planning an implantoprosthodontic procedure based on CBCT with the use of FEM: a) distribution of bone density in the area of implant application along the indicated line, b) virtual implant, c) model of the mandible with the arrangement of implants.

Occlusal analysis and numerical simulation of load distribution can also be performed, which is a challenge for modern clinical procedures [34]. An even greater challenge is the indication, using FEM, of functional disorders of the SS, especially in the temporomandibular joints [35].

More and more reports in the orthodontic area are aimed at evaluating the morphological status of the jaw and mandible in terms of malocclusion [36, 37]. Spatial mapping of the jaw and mandible structures and shapes of the patient is a very valuable scientific and clinical indication in the planning and solution of a prosthetic structure in terms of its location and range, the selection of biomaterials and manufacturing technologies in dental prosthetics [38, 39]. It also allows, with the use of FEM, the construction of the strength to be considered under personalized conditions, taking into account the physiological capacity of the tissues under load. The spatial objective dimensions of the masticatory organ form the basis for the correlation of shape with the possibilities of generating forces that may occur in occlusion [40–42].

Numerical simulations applying FEM used in orthodontics allow for determining biomechanical indications and prediction of the effects of therapy [43]. Using the CBCT, we performed a numerical simulation of the transfer of intrusive loads from the orthodontic arch through the bracket to the alveolar process. The study was carried out using a Kodak K9000 camera with high resolution (voxel with a size of 0.076 mm) in the dicom standard. The reduced stresses and the resultant displacements were analyzed in the structure of the bracket, the connection of the bracket and the maxillary incisal tooth, the tissues of the tooth, the suspension apparatus, and the area of the alveolus. Diagnostic imaging of the stomatognathic system performed using the CBCT cone beam tomography method, in addition to the evaluation of anatomical structures, was used for preoperative treatment planning, including biomechanical analysis of the tissues of the masticatory organs (Fig. 10) [43].

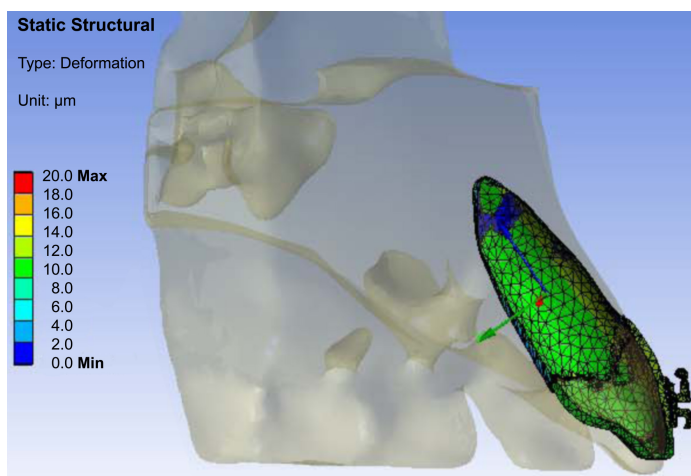


Fig. 10. Map of the displacement and deformation distribution in the area of incisor intrusion [43].

## 5. Conclusions

1. A comparison of pantomography and CBCT demonstrates that it is possible to determine the edge of the midsagittal plane in a pantomogram, but linear distances of even points and angle values deviate from reality due to the magnification and summation of the image and its flattening.
2. A comparison of lateral cephalometry and CBCT demonstrates that in cephalometry, linear measurements between odd points located in the midsagittal plane are reliable only if the natural scale in the plane is maintained. Other linear and angular dimensions are subject to error because of projecting distances and angles in one image plane, back projection, and image enlargement.
3. The metrological evaluation of the location of even points made on the basis of CBCT indicates asymmetry in the structures of the stomatognathic system.
4. CBCT has been shown to constitute an optimal basis for the geometric analysis of craniofacial bones. It makes it possible to determine multiplanar images, perform spatial reconstruction of an object, draw any cross-sectional plane, and perform a reliable biometric analysis. The main barrier to its application is the absence of criteria for diagnostic interpretation of the stomatognathic system developed for the population.

## Acknowledgements

The authors would like to thank Prof. Andrzej Ryniewicz from the State University of Applied Sciences in Nowy Sącz, Poland, for valuable metrological suggestions on the performed experiment.

## References

- [1] Al-Saleh, M. A., Alsufyani, N., Lai, H., Lagravere, M., Jaremko, J. L., & Major, P. W. (2017). Usefulness of MRI-CBCT image registration in the evaluation of temporomandibular joint internal derangement by novice examiners. *Oral Surgery, Oral Medicine, Oral Pathology and Oral Radiology*, 123(2), 249–256. <https://doi.org/10.1016/j.oooo.2016.10.016>

- [2] Codari, M., Caffini, M., Tartaglia, G. M., Sforza, C., & Baselli, G. (2017). Computer-aided cephalometric landmark annotation for CBCT data. *International Journal of Computer Assisted Radiology and Surgery*, 12(1), 113–121. <https://doi.org/10.1007/s11548-016-1453-9>
- [3] Míguez-Contreras, M., Jiménez-Trujillo, I., Romero-Maroto, M., López-de-Andrés, A., & Lagravère, M. O. (2017). Cephalometric landmark identification consistency between undergraduate dental students and orthodontic residents in 3-dimensional rendered cone-beam computed tomography images: A preliminary study. *American Journal of Orthodontics and Dentofacial Orthopedics*, 151(1), 157–166. <https://doi.org/10.1016/j.ajodo.2016.06.034>
- [4] Lee, S. Y., Choi, D. S., Jang, I., Song, G. S., & Cha, B. K. (2017). The genial tubercle: A prospective novel landmark for the diagnosis of mandibular asymmetry. *Korean Journal of Orthodontics*, 47(1), 50–58. <https://doi.org/10.4041/kjod.2017.47.1.50>
- [5] Daraze, A., Delatte, M., Saba, S. B., & Majzoub, Z. (2017). Craniofacial characteristics in the sagittal dimension: A cephalometric study in Lebanese young adults. *International Orthodontics*, 15(1), 114–130. <https://doi.org/10.1016/j.ortho.2016.12.001>
- [6] Heil, A., Gonzalez, E. L., Hilgenfeld, T., Kickingereeder, P., Bendszus, M., Heiland, S., Ozga, A. K., Sommer, A., Lux, Ch. J., & Zingler, S. (2017). Lateral cephalometric analysis for treatment planning in orthodontics based on MRI compared with radiographs: A feasibility study in children and adolescents. *PloS one*, e0174524. <https://doi.org/10.1371/journal.pone.0174524>
- [7] Kishimoto, T., Goto, T., Matsuda, T., Iwawaki, Y., & Ichikawa, T. (2022). Application of artificial intelligence in the dental field: A literature review. *Journal of Prosthodontic Research*, 66(1), 19–28. [https://doi.org/10.2186/jpr.JPR\\_D\\_20\\_00139](https://doi.org/10.2186/jpr.JPR_D_20_00139)
- [8] White, S. C., & Pharaoh, M. J. (2014). *Oral radiology, Principles and Interpretations*. St. Louis: Mosby.
- [9] Cobourne, M. T., & DiBiase, A. T. (2009). *Handbook of Orthodontics*, Mosby Elsevier, Edinburgh, London, New York, Oxford, Philadelphia, St Louis, Sydney, Toronto.
- [10] Siegel, J. A., McCollough, C. H., & Orton, C. G. (2017). Advocating for use of the ALARA principle in the context of medical imaging fails to recognize that the risk is hypothetical and so serves to reinforce patients' fears of radiation. *Medical Physics*, 44(1), 3–6. <https://doi.org/10.1002/mp.12012>
- [11] Sobieska, E., & Widmańska-Grzywaczewska, A. (2019). Cephalometry in orthodontic diagnostics – past and present. *Forum Ortodontyczne/Orthodontic Forum*, 15(2), 120–139. <https://doi.org/10.5114/for.2019.88346>
- [12] Ryniewicz, A., Ostrowska, K., Knapik, R., Ryniewicz, W., Krawczyk, M., Śladek, J., & Bojko, Ł. (2015). Evaluation of mapping of selected geometrical parameters in computer tomography using standards. *Przełqd Elektrotechniczny*, 91(6), 88–91. <https://doi.org/10.15199/48.2015.06.17>
- [13] Evaluation of measurement data – Guide to the expression of uncertainty in measurement – JCGM 100:2008.
- [14] Park, C. S., Park, J. K., Kim, H., Han, S. S., Jeong, H. G., & Park, H. (2012). Comparison of Conventional Lateral Cephalograms with Corresponding CBCT Radiographs. *Imaging Science in Dentistry*, 42(4), 201–205. <https://doi.org/10.5624/isd.2012.42.4.201>
- [15] Wang, R. H., Ho, C. T., Lin, H. H., & Lo, L. J. (2020). Three-dimensional cephalometry for orthognathic planning: Normative data and analyses. *Journal of the Formosan Medical Association*, 119(1), 191–203. <https://doi.org/10.1016/j.jfma.2019.04.001>
- [16] Pinheiro, M., Ma, X., Fagan, M. J., McIntyre, G. T., Lin, P., Sivamurthy, G., & Mossey, P. A. (2019). A 3D cephalometric protocol for the accurate quantification of the craniofacial symmetry and facial growth. *Journal of Biological Engineering*, 13(1), 42. <https://doi.org/10.1186/s13036-019-0171-6>

- [17] Jodeh, D. S., Kuykendall, L. V., Ford, J. M., Ruso, S., Decker, S. J., & Rottgers, S. A. (2019). Adding Depth to Cephalometric Analysis: Comparing Two- and Three-Dimensional Angular Cephalometric Measurements. *Journal of Craniofacial Surgery*, 30(5), 1568–1571. <https://doi.org/10.1097/SCS.0000000000005555>
- [18] Wang, M. F., Otsuka, T., Akimoto, S., & Sato, S. (2013). Vertical Facial Height and Its Correlation with Facial Width and Depth: Three Dimensional Cone Beam Computed Tomography Evaluation Based on Dry Skulls. *International Journal of Stomatology & Occlusion Medicine*, 6, 120–129. <https://doi.org/10.1007/s12548-013-0089-4>
- [19] Vernucci, R. A., Aghazada, H., Gardini, K., Fegatelli, D. A., Barbato, E., Galluccio, G., & Silvestri, A. (2019). Use of an anatomical mid-sagittal plane for 3-dimensional cephalometry: A preliminary study. *Imaging Science in Dentistry*, 49(2), 159–169. <https://doi.org/10.5624/isd.2019.49.2.159>
- [20] Yousefi, F., Rafiei, E., Mahdian, M., Mollabashi, V., Saboonchi, S. S., & Hosseini, S. M. (2019). Comparison efficiency of posteroanterior cephalometry and cone-beam computed tomography in detecting craniofacial asymmetry: A systematic review. *Contemporary Clinical Dentistry*, 10(2), 358. [https://doi.org/10.4103/ccd.ccd\\_397\\_18](https://doi.org/10.4103/ccd.ccd_397_18)
- [21] Ramirez-Sotelo, L. R., Almeida, S., Ambrosano, G. M., & Boscolo, F. (2012). Validity and Reproducibility of Cephalometric Measurements Performed in Full and Hemifacial Reconstructions Derived from Cone Beam Computed Tomography. *The Angle Orthodontist*, 82(5), 827–832. <https://doi.org/10.2319/072711-473.1>
- [22] Nur, M., Kayipmaz, S., Bayram, M., Celikoglu, M., Kilkis, D., & Sezgin, O. S. (2012). Conventional Frontal Radiographs Compared with Frontal Radiographs Obtained from Cone Beam Computed Tomography. *The Angle Orthodontist*, 82(4), 579–584. <https://doi.org/10.2319/080311-488.1>
- [23] Shibata, M., Nawa, H., Kise, Y., Fuyamada, M., Yoshida, K., Katsumata, A., Arijii, E., & Goto, S. (2012). Reproducibility of Three-Dimensional Coordinate Systems Based on Craniofacial Landmarks: A Tentative Evaluation of Four Systems Created on Images Obtained by Cone-Beam Computed Tomography with a Large Field of View. *The Angle Orthodontist*, 82(5), 776–784. <https://doi.org/10.2319/102511-662.1>
- [24] Hoff, M. N., Zamora, D., Spiekerman, C., Aps, J. K., Bollen, A. M., Herring, S. W., & Katz, F. (2019). Can cephalometric parameters be measured reproducibly using reduced-dose cone-beam computed tomography? *Journal of the World Federation of Orthodontists*, 8(2), 43–50. <https://doi.org/10.1016/j.ejwf.2019.02.006>
- [25] Ren, R., Luo, H., Su, C., Yao, Y., & Liao, W. (2021). Machine learning in dental, oral and craniofacial imaging: a review of recent progress. *PeerJ*, 9, e11451. <https://doi.org/10.7717/peerj.11451>
- [26] Kim, H., Son, T. G., Cho, H., Shim, E., Hwang, B. Y., Lee, J. W., & Kim, Y. (2020). Automated maxillofacial reconstruction software: development and evaluation. *Computer Methods in Biomechanics and Biomedical Engineering: Imaging & Visualization*, 8(2), 115–125. <https://doi.org/10.1080/21681163.2019.1608308>
- [27] Sam, A., Currie, K., Oh, H., Flores-Mir, C., & Lagravere-Vich, M. (2019). Reliability of different three-dimensional cephalometric landmarks in cone-beam computed tomography: A systematic review. *The Angle Orthodontist*, 89(2), 317–332. <https://doi.org/10.2319/042018-302.1>
- [28] Zamora, N., Cibrian, R., Gandia, J. L., & Paredes, V. (2013). Study between Anb Angle and Wits Appraisal in Cone Beam Computed Tomography (CBCT). *Medicina Oral, Patología Oral y Cirugía Bucal*, 18(4), 725–732. <https://doi.org/10.4317/medoral.18919>
- [29] Abdi, A. H., Pesteie, M., Prisman, E., Abolmaesumi, P., & Fels, S. (2019). *Variational Shape Completion for Virtual Planning of Jaw Reconstructive Surgery*. In International Conference on Medical Image Computing and Computer-Assisted Intervention. Springer, Cham, 227–235. [https://doi.org/10.1007/978-3-030-32254-0\\_26](https://doi.org/10.1007/978-3-030-32254-0_26)

- [30] Husain, K., Rashid, M., Vitković, N., Mitić, J., Milovanović, J., & Stojković, M. (2018). Geometrical models of mandible fracture and plate implant. *Facta Universitatis, Series: Mechanical Engineering*, 16(3), 369–379. <https://doi.org/10.22190/FUME170710028H>
- [31] Aljehani, D. (2022). Review of the Impact of Mandibular Setback Surgery for the Correction of Class III Malocclusion on the Upper Airway Space. *Dentistry Review*, 100033. <https://doi.org/10.1016/j.dentre.2022.100033>
- [32] Ryniewicz, W., Ryniewicz, A., & Bojko, Ł. (2019). Geometrical parameters of the mandible in 3D CBCT imaging. *Biocybernetics and Biomedical Engineering*, 39(2), 301–311. <https://doi.org/10.1016/j.bbe.2018.09.005>
- [33] Husain, K. N., Stojković, M., Vitković, N., Milovanović, J., Trajanović, M., Rashid, M., & Milovanović, A. (2019). Procedure for creating personalized geometrical models of the human mandible and corresponding implants. *Tehnički vjesnik*, 26(4), 1044–1051. <https://doi.org/10.17559/TV-20181009193111>
- [34] Liu, X., Pang, F., Li, Y., Jia, H., Cui, X., Yue, Y., Yang, X., & Yang, Q. (2019). Effects of Different Positions and Angles of Implants in Maxillary Edentulous Jaw on Surrounding Bone Stress under Dynamic Loading: A Three-Dimensional Finite Element Analysis. *Computational and Mathematical Methods in Medicine*. <https://doi.org/10.1155/2019/8074096>
- [35] Kim, J. H., Park, H. J., & Ryu, J. W. (2021). Association between Temporomandibular Disorder and Masticatory Muscle Weakness: A Case report. *Journal of Oral Medicine and Pain*, 46(4), 155–160. <https://doi.org/10.14476/jomp.2021.46.4.155>
- [36] Toro-Ibacache, V., Ugarte, F., Morales, C., Eyquem, A., Aguilera, J., & Astudillo, W. (2019). Dental malocclusions are not just about small and weak bones: assessing the morphology of the mandible with cross-section analysis and geometric morphometrics. *Clinical Oral Investigations*, 23(9), 3479–3490. <https://doi.org/10.1007/s00784-018-2766-6>
- [37] Orhan, K., & Görürgöz, C. (2021). USG Imaging in Orthodontics. *Ultrasonography in Dentomaxillo-facial Diagnostics* pp. 227–249. Springer, Cham. [https://doi.org/10.1007/978-3-030-62179-7\\_15](https://doi.org/10.1007/978-3-030-62179-7_15)
- [38] Ryniewicz, W. (2008). *Modeling and structural optimization of prosthetic bridges in the mandibular lateral segment*. [Doctoral dissertation, Jagiellonian University Medical College].
- [39] Ryniewicz, W., Ryniewicz, A. M., & Bojko, Ł. (2016). The effect of a prosthetic crown's design on the accuracy of mapping an abutment teeth's shape. *Measurement*, 91, 620–627. <https://doi.org/10.1016/j.measurement.2016.05.019>
- [40] Buezas, G. N., Becerra, F., Echeverría, A. I., Cisilino, A., & Vassallo, A. I. (2019). Mandible strength and geometry in relation to bite force: a study in three caviomorph rodents. *Journal of Anatomy*, 234(4), 564–575. <https://doi.org/10.1111/joa.12946>
- [41] Schaeffer, J., Benton, M. J., Rayfield, E. J., & Stubbs, T. L. (2019). Morphological disparity in theropod jaws: comparing discrete characters and geometric morphometrics. *Palaeontology*, 63(2), 283–299. <https://doi.org/10.1111/pala.12455>
- [42] Sella-Tunis, T., Pokhojaev, A., Sarig, R., O'Higgins, P., & May, H. (2018). Human mandibular shape is associated with masticatory muscle force. *Scientific Reports*, 8(1), 1–10. <https://doi.org/10.1038/s41598-018-24293-3>
- [43] Ryniewicz, W., Ryniewicz, A. M., Bojko, Ł., Pełka, P., Filipek, J., Williams, S., & Loster, B. W. (2016). Three-dimensional finite element simulation of intrusion of the maxillary central incisor. *Biocybernetics and Biomedical Engineering*, 36(2), 385–390. <https://doi.org/10.1016/j.bbe.2016.02.003>



**Wojciech Ryniewicz** is an Assistant Professor at the Department of Prosthodontics and Orthodontics, Faculty of Medicine, Collegium Medicum of the Jagiellonian University. His scientific interests include numerical modeling, biomechanics of the stomatognathic system using the finite element method, prosthetics of fixed dental restorations.



**Anna M. Ryniewicz** is Professor at the Faculty of Mechanical Engineering and Robotics of the AGH University of Science and Technology (and head of the Laboratory of Material Science and Technology of Dental Biomaterials, Jagiellonian University Medical College). Her research activities focus on bioengineering, biomechanics, biomaterials, 3D reconstruction of diagnostic imaging, measurements in medicine.



**Łukasz Bojko** is an Assistant Professor at the Faculty of Mechanical Engineering and Robotics at the AGH University of Science and Technology. His research areas of research interest are optical coordinate metrology, application of new technologies in materials for medical applications, technology of laser sintering of metal powders, bioengineering structures.